J Nanostruct 16(2): 2087-2096, Spring 2026

RESEARCH PAPER

Box–Behnken Optimization of a Probe-Ultrasonicated Paracetamol Nanosuspension: Colloidal Characterization and Dissolution Enhancement

Mohammed Sattar [1,2] *, *Malathe Alshawi* [1], *Neven Nsaif Jasim* [1]

[1] *Department of Pharmaceutics, College of Pharmacy, University of Basrah, Basrah, Iraq*

[2] *Department of Pharmacy, Alfarqadein University College, Basrah, Iraq*

ARTICLE INFO

Article History:
Received 03 December 2025
Accepted 19 March 2026
Published 01 April 2026

Keywords:
Box–Behnken design
Carbopol 71G NF
Dynamic light scattering
Nanosuspension
Paracetamol
Probe ultrasonication

ABSTRACT

Generally conventional paracetamol suspensions contain coarse particles (10–90 μm) that sediment rapidly. This has a risk of dose variability in successive dose during usage; especially, paracetamol is given to children on basis of weight to avoid liver toxicity. In this work, suspension of paracetamol was prepared at nano level by ultrasonication method and stabilized by Carbopol 71G NF and poly sorbate 80. The resultant nano scale suspension was evaluated to produce stable nanosuspension in physical and dissolution terms. A three-factor, three-level Box–Behnken design (BBD) address the effects of Carbopol 71G NF (X_1), Polysorbate 80 (X_2) and sonication amplitude (X_3) on Z-average diameter (Y_1), polydispersity index (Y_2) and zeta potential (Y_3). All three quadratic models were significant ($R^2 \geq 0.95$; $p < 0.0001$); Carbopol was the dominant variable, and the $X_1 \times X_3$ interaction was significant ($p < 0.05$). Desirability optimization (D = 0.847) identified 0.38% w/v Carbopol, 0.062% w/v Polysorbate 80, and 48% amplitude, and the validation batch matched predictions within 2% (341 ± 12 nm; PDI 0.186; zeta potential −29.7 mV). HPLC content (22.93 ± 0.75 mg mL^{-1}) comply well with limits in USP. The optimized formula released 92.4% of the dose within 15 min against 69.8% for unprocessed powder (f_2 = 31.7) HCl (pH=1.2). The formulation was physically and chemically unchanged after 21 days at −4, 24, and 40 °C. The Carbopol–Polysorbate 80 electrostatic network preserved colloidal integrity, and the BBD exposed a Carbopol–amplitude synergy that one-variable-at-a-time screening cannot detect.

How to cite this article
Sattar M., Alshawi M., Nsaif Jasim N. Box–Behnken Optimization of a Probe-Ultrasonicated Paracetamol Nanosuspension: Colloidal Characterization and Dissolution Enhancement. J Nanostruct, 2026; 16(2):2087-2096. DOI: 10.22052/JNS.2026.02.055

INTRODUCTION

Paracetamol is the first-line analgesic-antipyretic in children under six because aspirin is contraindicated owing to the risk of Reye's syndrome [1]. Generally, the pediatric dose of paracetamol is 15mg/Kg q.i.d. because children below five years cannot swallow solid dosage forms, so oral liquids are the only practical option. Accordingly, as much as uniformly distributed liquid system, the safer precise dose given [2]. The dose accuracy is achieved by uniform distribution of medicine in that particular milliliters -dose given

* *Corresponding Author Email: mohammed.jabbar@uobasrah.edu.iq*

to the patient. The main factor that determines available number of particles of medicine in each dose is sedimentation rate. as long as the sedimentation time, the more chance for accurate dose given to the patient. Stokes' law predicts that sedimentation velocity proportionally increases with increase in radius of particles. That means as the size of particle reduces, the time for particles to sediment would take longer time return to its original non distributed resting state before agitation. This longer time achiever allows more time for dose pouring from bottle into the spoon or dosing device. Thus, more uniform dose would be achieved. The conventional method for preparation of paracetamol produces microscale suspended particles'; 10–90 µm. Which settles within minutes, producing a concentration gradient along the height of the bottle [3]. Nanosuspension approach, which is a colloidal dispersion of drug crystals has particle size below 1 µm that stabilized by polymers and surfactants can improve both instability and slow dissolution. Below 1 µm, Brownian diffusion counteract settling effect of gravity. Beside that, the Ostwald–Freundlich equation suggest that a reduced particle size increase saturated solubility and improve the dissolution profile [4].

Paracetamol belongs to BCS Class I/III boundary. It is well absorbed once dissolved [5]. however, coarse suspended particles, as a role of thumb, has a lower dissolution rate than nano size comparator.

Probe ultrasonication generates acoustic cavitation at 20 kHz. The collapse of microbubbles produces shock waves and shear that fracture crystals into nanoparticles [6]. Cavitation requires a low-viscosity medium, so a two-step process is essential, sonication in a dilute surfactant solution firstly. Which followed by incorporation into the polymer vehicle. Therefore, particle size depends on sonication energy in first step and on polymer surface coverage in the second step.

In this study the combined effect of these two variables were evaluated statically [7]. Box–Behnken design (BBD) evaluates three factors at three levels in 15–16 runs, resolving main effects, interactions, and curvature [8,9]. Alshweiat et al. [10] applied BBD to indomethacin nanosuspensions and identified stabilizer concentration and sonication power as the dominant variables. Boscolo et al. [7] confirmed that these factors account for >95% of the particle-size variance of ursodeoxycholic acid nanosuspensions. Wang et al. [11] achieved 303.7 nm, PDI 0.178, and −31.10 mV for breviscapine using the same approach.

Carbopol 71G NF is a granular carbomer (MW > 3×10^9 Da) that disperses in water to form a partially ionized polyacrylic acid network functioning simultaneously as rheology modifier and colloidal stabilizer [12]. At pH circa 5 polyacrylic acid network provide electrostatic stabilization via the ionized carboxylate groups that generate electrostatic repulsion, and the extended chains that yield steric hindrance [13,14]. Polysorbate 80 improves wetting of hydrophobic crystal surface and facilitates Carbopol adsorption. Therefore, a synergistic effect would be expected from combined corporations [4].

This study depends on a three-factor BBD to optimize Carbopol 71G NF (X_1), Polysorbate 80 (X_2), and sonication amplitude (X_3) with respect to particle size (Y_1), PDI (Y_2), and zeta potential (Y_3). The optimized formulation was then characterized by dissolution, rheology, HPLC content uniformity, and 21-day stability testing.

MATERIALS AND METHODS

Materials

Paracetamol BP (≥99.5%) was identity-verified by ATR-FTIR. Carbopol 71G NF (Lubrizol, Surfachem Group Ltd, UK), Polysorbate 80 (BDH Chemicals), disodium EDTA, sodium saccharin, methyl paraben, and propyl paraben (Sigma-Aldrich), sucrose BP, sorbitol 70% w/v (Sigma-Aldrich), carmoisine solution (1% w/v, prepared in-house), and strawberry flavor (Bush Boake Allen). Methanol and acetonitrile were HPLC-grade (Fisher Scientific), and water was freshly prepared.

ATR-FTIR Drug Identity

ATR-FTIR spectra (PerkinElmer Spectrum 400; 4000–650 cm^{-1}; 4 cm^{-1} resolution) were compared with the library reference; a concordance score ≥97% confirmed identity.

Base Formulation

All 16 formulations were made in the same dispersion medium (Table 1); only Carbopol (X_1) and Polysorbate 80 (X_2) were varied. The composition was adapted from the Lubrizol PABSMOL platform [15], with probe ultrasonication replacing sieving.

The vehicle was prepared in three Parts; Part A (Carbopol dispersed in the sweetener/EDTA solution at <800 rpm). Part B (sucrose, sorbitol, and

parabens dissolved at 70 °C, pH adjusted to 4.9–5.0 with 10% NaOH). Finally, Part C (Polysorbate 80 and paracetamol triturated in 50 mL water).

Box–Behnken Experimental Design

A three-factor, three-level BBD (Design-Expert v.13, Stat-Ease) generated 16 runs (15 + 1 center-point replicate). Factor levels as in Table 2 were derived from preliminary experiments. The responses were Y_1 = Z-average diameter, Y_2 = PDI, and Y_3 = zeta potential. A full second-order polynomial was fitted by least-squares. Model significance was assessed by ANOVA ($p < 0.05$), and desirability optimization minimized Y_1 and Y_2 while maximizing Y_3.

Nanosuspension Preparation

To reduce size, the low-viscosity aqueous medium, Part C pre-dispersion, to ensured unimpeded cavitation, was subjected to probe-ultrasonicated (Biobase, Germany). The ultrasonication were pulsed 5 sec. on followed by 5 second off for 10 min active time. The mixture was kept in ice bath at <30 °C along sonication process at the BBD-prescribed amplitude in Table 2.

Then the nanosuspension was incorporated into the Carbopol vehicle, Parts A and Part B, at 300 rpm for 15 min. The low shear preserved the gel network, and Carbopol chains adsorbed onto the nanoparticle surfaces that forming the electrostatic coating that governs all three DLS results. Color, flavor, and water were then added to 300 g. All batches were prepared and characterized on the same day.

Dynamic Light Scattering

Particle size, PDI, and zeta potential were measured by Malvern Zetasizer Nano series (Malvern Instruments, UK) at 25 ± 0.1 °C. Each samples were diluted 100 times in deionized water. All measurements were performed in triplicate and the average was taken ± SD.

Characterization of the Optimized Formulation
Rheometry

Cone-and-plate rheometry used a Thermo HAAKE RheoWin (2°/35 mm cone; 25 ± 0.1 °C). A

Table 1. Base vehicle composition for all 16 BBD formulations.

Component	Function	Amount/300 ml
Paracetamol BP	API	7.2 g
Carbopol 71G NF	Stabilizer/rheology modifier	Variable (X_1)
Polysorbate 80	Wetting agent	Variable (X_2)
Disodium EDTA	Chelating agent	0.15 g
Sodium saccharin	Sweetener	0.45 g
Sucrose BP	Bulk sweetener	150 g
Sorbitol 70% w/v	Humectant	37.5 ml
Methyl paraben	Preservative	0.60 g
Propyl paraben	Preservative	0.06 g
NaOH 10% w/v	pH adjustment	q.s.
Carmoisine 1% w/v	Colorant	0.6 ml
Strawberry flavor	Flavoring	1.5 g
Deionized water	Vehicle	q.s. to 300 g

Table 2. Independent variables and coded levels.

Factor	Variable	Low (−1)	Center (0)	High (+1)
X_1	Carbopol 71G NF (% w/v)	0.15	0.30	0.45
X_2	Polysorbate 80 (% w/v)	0.025	0.050	0.075
X_3	Sonication amplitude (%)	20	40	60

shear stress rate from 0 to 300 s^{-1} and back to 0 s^{-1} was applied. Yield stress was measured at the viscosity inflection and limiting viscosity from the plateau above 240 s^{-1}. Day-21 stability samples were tested under identical conditions.

HPLC Content Uniformity

Reversed-phase HPLC was performed on a Beckman System Gold (Fortis C18, 5 µm, 150 × 4.6 mm; 25% methanol; 1.0 mL min^{-1}; 254 nm; retention time 3.0 ± 0.1 min). A five-point calibration were measured from 10 to100 µg mL^{-1} with LOD = 3.3σ/S, and LOQ = 10σ/S. triplicates samples were withdrawn from the top, middle, and bottom of each bottle (after five shakes); each sample was of 1g of final formulation. The recovered paracetamol concentration was weight against the acceptance range in USP, 90.0–110.0% of the claimed concertation.

Dissolution

Dissolution was done by using USP Apparatus

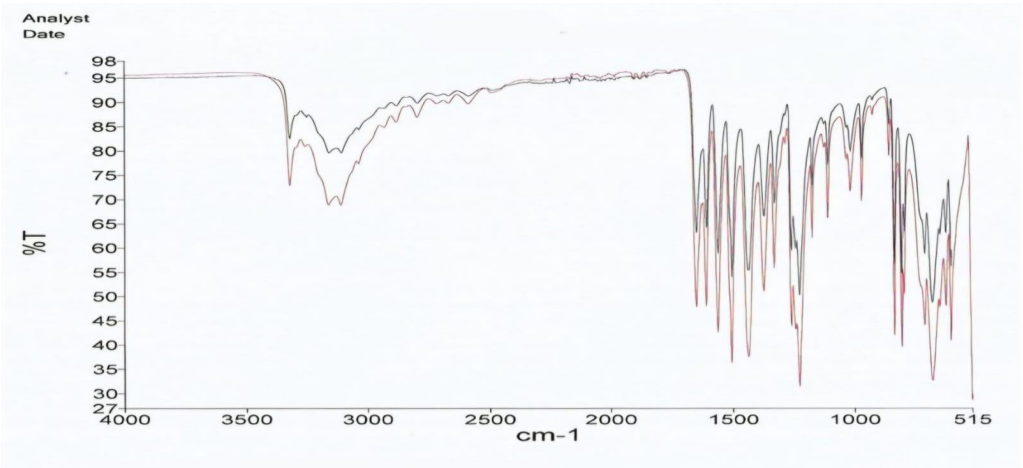

Fig. 1. ATR-FTIR spectrum of paracetamol raw material overlaid on the library reference. Concordance 99%; diagnostic bands annotated.

Table 3. BBD matrix and DLS responses (mean ± SD, n = 3). CP = center-point; Val. = validation.

Run	X_1	X_2	X_3	Y_1 (nm)	Y_2	Y_3 (mV)
F1	0.15	0.025	40	712 ± 28	0.387 ± 0.031	−18.3 ± 2.1
F2	0.45	0.025	40	398 ± 19	0.241 ± 0.022	−28.4 ± 1.8
F3	0.15	0.075	40	586 ± 24	0.319 ± 0.027	−22.7 ± 1.9
F4	0.45	0.075	40	321 ± 15	0.198 ± 0.018	−31.2 ± 1.6
F5	0.15	0.050	20	641 ± 31	0.351 ± 0.029	−20.1 ± 2.3
F6	0.45	0.050	20	449 ± 21	0.268 ± 0.024	−26.8 ± 1.7
F7	0.15	0.050	60	498 ± 22	0.294 ± 0.025	−21.9 ± 2.0
F8	0.45	0.050	60	303 ± 14	0.189 ± 0.017	−30.1 ± 1.5
F9	0.30	0.025	20	531 ± 25	0.307 ± 0.028	−23.4 ± 1.9
F10	0.30	0.075	20	487 ± 23	0.278 ± 0.024	−25.6 ± 1.8
F11	0.30	0.025	60	412 ± 18	0.247 ± 0.021	−26.1 ± 1.7
F12	0.30	0.075	60	374 ± 17	0.223 ± 0.019	−27.9 ± 1.6
F13 (CP)	0.30	0.050	40	362 ± 16	0.214 ± 0.018	−28.8 ± 1.5
F14 (CP)	0.30	0.050	40	268 ± 12	0.156 ± 0.014	−33.6 ± 1.4
F15 (CP)	0.30	0.050	40	351 ± 15	0.209 ± 0.018	−29.4 ± 1.6
F16 (Val.)	0.38	0.062	48	341 ± 12	0.186 ± 0.019	−29.7 ± 1.6

II (Erweka DT 720) at 50 rpm; 37.0 ± 0.5 °C; 900 mL HCl, pH 1.2. aliquots from optimized nanosuspension versus plain paracetamol powder were done in triplicates (n=3) at 5, 10, 15, 30, 45, 60, and 120 min with volume replacement. the released paracetamol was measured in each sample using HPLC and DE_{15}, DE_{60}, and f_2 were calculated.

Stability

A 10 mL sample were stored in amber vials at 4, 24, and 40 °C for 21 days. DLS and HPLC were performed on days 0, 7, and 21, and rheology where done on day 0 and 21 only.

Statistical Analysis

All data are reported as mean of n=3 ± SD unless otherwise stated. One-way ANOVA with Tukey post-hoc (SPSS v.26) was used with $p < 0.05$ was taken as significant.

RESULTS AND DISCUSSION

Drug Identity (ATR-FTIR)

The paracetamol spectrum matched the library reference at 99% concordance (Fig. 1), exceeding the 97% threshold. Diagnostic bands were identified at 3324 and 3163 cm^{-1} (N–H/O–H stretch), 1654 cm^{-1} (amide I C=O), 1610 and 1506 cm^{-1} (aromatic C=C), and 1259 cm^{-1} (aryl C–O), with no extraneous peaks. The pattern is consistent with monoclinic Form I [5].

BBD Responses

All 16 runs yielded submicron particles as shown in Table 3. Z-average 268–712 nm, PDI 0.156–0.387, and zeta potential −18.3 to −33.6 mV. The center-point replicates (F13–F15) gave 327 ± 47 nm (RSD 14.4%). This might reflect the cavitation variability characteristic of laboratory scale ultrasonication. Tripling Carbopol from 0.15% to 0.45% reduced particle size by 30–45% which shows an effect no other variable provided.

ANOVA and Model Interpretation

Significant quadratic models were confirmed for all three responses ($p < 0.0001$; Table 4) along with lack of fit was non-significant in every case ($p > 0.05$). The factor effect order, Carbopol >

Table 4. ANOVA summary. ns = not significant.

Source	Y_1 F	Y_1 p	Y_2 F	Y_2 p	Y_3 F	Y_3 p
Model	38.47	<0.0001	29.84	<0.0001	23.17	<0.0001
X_1	218.63	<0.0001	163.49	<0.0001	141.82	<0.0001
X_2	26.41	0.0013	19.07	0.0032	14.53	0.0067
X_3	57.82	<0.0001	44.31	<0.0001	38.94	0.0002
X_1X_2	3.14	0.12 ns	2.87	0.13 ns	2.19	0.18 ns
X_1X_3	8.72	0.021	7.63	0.029	6.41	0.040
X_2X_3	1.84	0.22 ns	1.52	0.26 ns	1.18	0.31 ns
X_1^2	12.36	0.010	9.84	0.017	8.21	0.024
X_3^2	7.54	0.029	6.12	0.043	5.03	0.060
Lack of fit	2.31	0.22 ns	1.98	0.24 ns	1.74	0.27 ns

Statistic	Y_1	Y_2	Y_3
R^2	0.9741	0.9612	0.9503
Adj. R^2	0.9366	0.9091	0.8852
Pred. R^2	0.8617	0.8243	0.7941
Adeq. precision	21.34	18.67	16.29

Table 5. Model prediction vs. experimental validation (F16).

Response	Predicted	Observed (n=3)	Error (%)
Y_1 (nm)	338	341 ± 12	0.9
Y_2 (PDI)	0.189	0.186 ± 0.019	1.6
Y_3 (mV)	−30.1	−29.7 ± 1.6	1.3

amplitude > Polysorbate 80, was consistent across responses. F-value for Carbopol was =218.63 for Y_1. This value was four times that of amplitude (57.82) and eight times that of Polysorbate 80 (26.41). it went well with the ranking reported by Alshweiat et al. for indomethacin [10].

The $X_1 \times X_3$ interaction ($p \leq 0.04$ for every response) could be attributed to ultrasonication amplitude that cause fragmentation in the first step that generate greater surface area which must be covered by Carbopol in the second step to prevent re-aggregation. At 0.15% of Carbopol, increasing the amplitude from 20% to 60% reduced size by 22%. At 0.45% Carbopol, the same change achieved 33%. This synergy is undetectable by one-variable-at-a-time screening.

Significant X_1^2 and X_3^2 terms indicate diminishing returns, placing both optima inside the design space. Excess Carbopol increase viscosity without improving coverage. Also excess amplitude induces local heating and Ostwald ripening between pulses [16]. The coded equations are for the free factors:

$$Y_1 = 327.0 - 134.8X_1 - 47.2X_2 - 69.4X_3 - 21.6X_1X_2 - 38.7X_1X_3 - 16.2X_2X_3 + 42.3{X_1}^2 + 18.6{X_2}^2 + 29.4{X_3}^2$$

$$Y_2 = 0.193 - 0.073X_1 - 0.026X_2 - 0.038X_3 - 0.019X_1X_2 - 0.031X_1X_3 - 0.014X_2X_3 + 0.023{X_1}^2 + 0.014{X_2}^2 + 0.019{X_3}^2$$

$$Y_3 = -30.6 + 7.21X_1 + 2.49X_2 + 3.74X_3 + 1.69X_1X_2 + 3.01X_1X_3 + 1.24X_2X_3 - 2.18{X_1}^2 - 1.38{X_2}^2 - 1.82{X_3}^2$$

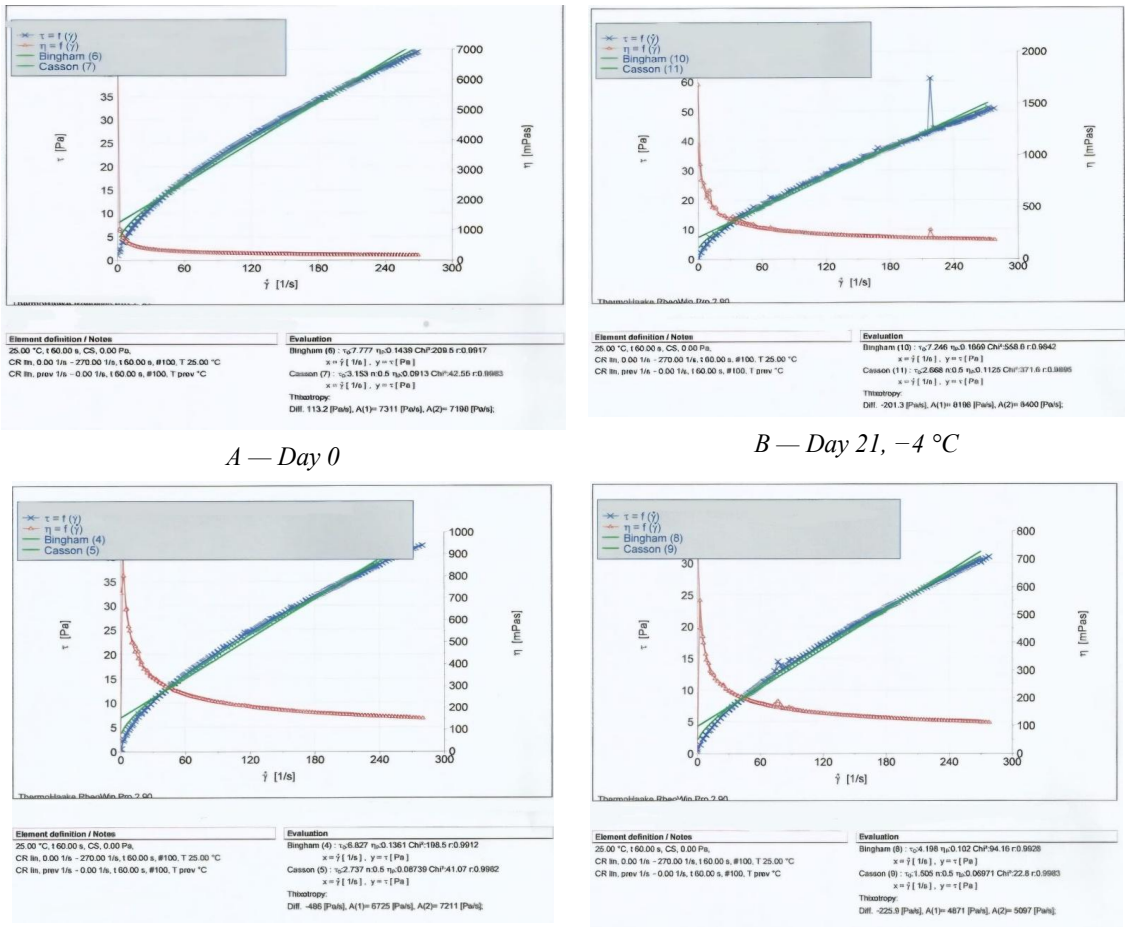

A — Day 0 *B — Day 21, −4 °C*

C — Day 21, 24 °C *D — Day 21, 40 °C*

Fig. 2. Cone-and-plate rheograms at day 0 (A) and at day 21 after storage at −4 °C (B), 24 °C (C), and 40 °C (D). Filled symbols = ascending ramp; open symbols = descending ramp. The superimposition of the curves confirms the absence of thixotropy and rheological stability.

Optimized Formulation

Desirability optimization (D = 0.847) identified X_1 = 0.38%, X_2 = 0.062%, and X_3 = 48%. The validation batch (F16) returned 341 ± 12 nm, PDI 0.186, and −29.7 mV as in Table 5. The error in prediction was 0.9%, 1.6%, and 1.3% for all, which was less than the acceptance level ;i.e, <10% [17].

X_1 at 0.38% (between center and upper level) reflects the diminishing returns imposed by the X_1^2 curvature. X_3 at 48% (near the central level) confirms an interior optimum created by thermal ripening at high power. The zeta potential of −29.7 mV indicates adequate electrostatic stabilization [18]. Whereases, PDI of 0.186 indicates the absence of large aggregates. These values go well with findings by Wang et al. [11] (303.7 nm, 0.178, −31.10 mV) and Boscolo et al. [7].

Rheological Properties

The day-0 rheogram (Fig. 2A) revealed Bingham plastic flow with a yield stress of ≈9.8 Pa and a limiting viscosity of ≈200 mPa·s. The ascending and descending curves were superimposable, indicating no thixotropy. At 341 nm, Brownian motion dominates over gravity, and the yield stress provides supplementary restraint. The gravitational shear exerted by a particle is ~10^{-4} Pa, well below threshold. Varges et al. [13] states the functional range at 2–20 Pa. Dinkgreve et al. [14] demonstrated that Carbopol exhibit thixotropic under high-speed mixing. however, a rotation speed less than 800 rpm adopted in this test preserved non-thixotropic behavior. Day-21 rheograms at every storage condition were superimposable on day 0. From Fig. 2B–D, the yield

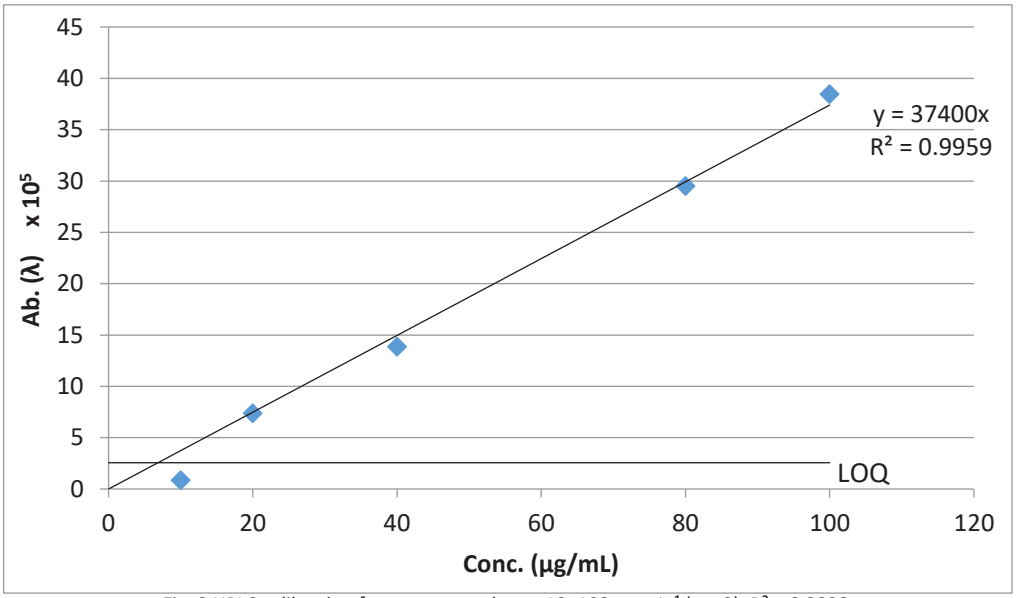

Fig. 3 HPLC calibration for paracetamol over 10–100 µg mL^{-1} (n = 3). R^2 = 0.9998.

Table 6. HPLC calibration accuracy (n = 3).

Conc. (µg/ml)	Peak area	Back-calc.	Accuracy (%)
10	376,847	10.05	100.5
20	746,319	19.93	99.7
40	1,500,214	40.09	100.2
80	2,985,443	79.80	99.8
100	3,749,912	100.24	100.2

stress and viscosity changed by <4% ($p > 0.05$).

HPLC Calibration and Content Uniformity

Calibration was linear across 10–100 µg mL^{-1} (R^2 = 0.9998; Fig. 3), with LOD = 0.768 µg mL^{-1} and LOQ = 2.56 µg mL^{-1}. System precision (RSD = 0.69%, n = 3 at 40 µg mL^{-1}) met the ICH Q2(R2) criteria [19].

The mean drug content was 22.93 ± 0.75 mg mL^{-1}, corresponding to 95.5 ± 3.1% of the 24 mg mL^{-1} nominal (Table 7); all samples were within the USP limits of 90.0–110.0%. The low inter-sample

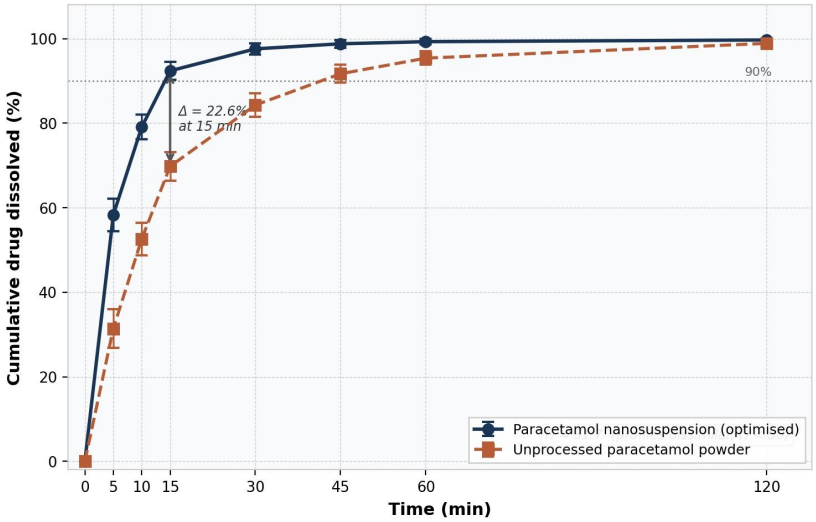

Fig. 4. Dissolution profiles in simulated gastric fluid (pH 1.2, 37 °C, n = 3). Nanosuspension (●) vs. unprocessed powder (□); f_2 = 31.7.

Table 7. Content uniformity (n = 3). Nominal: 24 mg mL^{-1}.

Sample	Peak area	Content (mg/ml)	Recovery (%)	USP
Top	2,065,392	22.08	92.0	Yes
Middle	2,200,967	23.53	98.0	Yes
Bottom	2,168,242	23.18	96.6	Yes
Mean ± SD	2,144,867 ± 71,316	22.93 ± 0.75	95.5 ± 3.1	—

Table 8. Dissolution data (n = 3, mean ± SD).

Time (min)	Nanosuspension (%)	Powder (%)	Δ (%)
5	58.3 ± 3.8	31.4 ± 4.6	26.9
10	79.1 ± 2.9	52.6 ± 3.9	26.5
15	92.4 ± 2.1	69.8 ± 3.4	22.6
30	97.6 ± 1.3	84.3 ± 2.8	13.3
45	98.8 ± 0.9	91.7 ± 2.1	7.1
60	99.3 ± 0.6	95.4 ± 1.6	3.9
120	99.7 ± 0.4	98.9 ± 0.8	0.8
DE_{15}	81.6	53.7	—
DE_{60}	95.1	83.6	—
f_2	—	31.7	Dissimilar

Table 9. HPLC stability (mg mL^{-1}).

Condition	Day 0	Day 7	Day 21	USP
−4 °C	22.93	23.08	23.01	Within
24 °C	22.93	22.89	22.78	Within
40 °C	22.93	23.97	24.41	Within

Table 10. DLS stability (mean ± SD, n = 3).

Cond.	Day 0	Day 7	Day 21	PDI	ZP (mV)	Δ (%)
−4 °C	341±12	354±14	368±17	0.208±0.021	−28.4±1.9	+7.9
24 °C	341±12	349±13	358±15	0.196±0.020	−29.1±1.7	+5.0
40 °C	341±12	361±16	372±21	0.231±0.024	−27.6±2.1	+9.1

RSD of 3.3% confirms uniform drug distribution hich clearly and advantage of e nanometric particle size, which prevents sedimentation via gravity.

Dissolution

At 15 min the nanosuspension released 92.4 ± 2.1% of the dose, against 69.8 ± 3.4% for the unprocessed powder (Fig. 4; Table 8; f_2 = 31.7, profiles dissimilar). Both formulations exceeded 95% release by 60 min. The ~117-fold increase in specific surface area (from ≈40 µm to 341 nm) accelerates dissolution per the Noyes–Whitney equation without altering equilibrium solubility [4].

The f_2 value of 31.7 is used here as a descriptive comparator. FDA/EMA compliance requires ≤3 time points above 85%, so application is limited. DE_{15} (81.6% vs. 53.7%) provides a single integrative measure of the early-phase advantage. Clinical conditions highlight caution that pediatric gastric conditions differ materially from the paddle apparatus [20]. However, the reproducible dissolution advantage supplies clear physicochemical properties for earlier effectiveness that might be expected.

Stability

HPLC content remained within the USP limits at every temperature over 21 days (Table 9; ANOVA: $F(2,6) = 2.14$, $p = 0.196$). No color change, phase separation, or pH shift greater than 0.2 units was observed.

DLS showed no significant changes over the 21 days (Table 10; $p > 0.05$). The maximum size increase was +9.1% at 40 °C, which is below the 15% instability threshold [21]. The sample stored at - 4 °C shows (+7.9%) grew; which slightly more than the 24 °C sample (+5.0%). It might be because the higher viscosity at low temperature slows Carbopol chain diffusion to the particle surface and transiently exposes crystal growth sites [22]. Zeta potential was preserved at every condition.

CONCLUSION

A Box–Behnken design successfully optimized a probe-ultrasonicated paracetamol nanosuspension, confirming that nanosized can improve physical stability and accelerate dissolution. Carbopol 71G NF was the main variable, and its interaction with sonication amplitude, which is invisible to single-variable screening, placed the optimum inside the design space (0.38% Carbopol, 0.062% Polysorbate 80, 48% amplitude; 341 nm, PDI 0.186, zeta potential −29.7 mV). The formulation released 92.4% of the dose within 15 min against 69.8% for coarse powder, USP limits for uniformity, and remained physically and chemically unchanged for 21 days at −4–40 °C. Future work should extend this screening with ICH Q1A(R2) long-term stability, dissolution in biorelevant media, preservative efficacy testing, and a pediatric pharmacokinetic study.

CONFLICT OF INTEREST

The authors declare that there is no conflict of interests regarding the publication of this manuscript.

REFERENCES

1. Thibault C, Pelletier É, Nguyen C, Trottier ED, Doré-Bergeron

M-J, DeKoven K, et al. The Three W's of Acetaminophen In Children: Who, Why, and Which Administration Mode? The Journal of Pediatric Pharmacology and Therapeutics. 2023;28(1):20-28.
2. Klingmann V, Vallet T, Münch J, Stegemann R, Wolters L, Bosse H-M, et al. Dosage Forms Suitability in Pediatrics: Acceptability of Analgesics and Antipyretics in a German Hospital. Pharmaceutics. 2022;14(2):337.
3. Gaikwad SS, Morales JO, Lande NB, Catalán-Figueroa J, Laddha UD, Kshirsagar SJ. Exploring paediatric oral suspension development: Challenges, requirements, and formulation advancements. Int J Pharm. 2024;657:124169.
4. Jacob S, Nair AB, Shah J. Emerging role of nanosuspensions in drug delivery systems. Biomaterials Research. 2020;24(1).
5. Kalantzi L, Reppas C, Dressman JB, Amidon GL, Junginger HE, Midha KK, et al. Biowaiver monographs for immediate release solid oral dosage forms: Acetaminophen (paracetamol). J Pharm Sci. 2006;95(1):4-14.
6. Pınar SG, Oktay AN, Karaküçük AE, Çelebi N. Formulation Strategies of Nanosuspensions for Various Administration Routes. Pharmaceutics. 2023;15(5):1520.
7. Boscolo O, Flor S, Salvo L, Dobrecky C, Höcht C, Tripodi V, et al. Formulation and Characterization of Ursodeoxycholic Acid Nanosuspension Based on Bottom-Up Technology and Box–Behnken Design Optimization. Pharmaceutics. 2023;15(8):2037.
8. Kumar R, Reji M. Response surface methodology (RSM): An overview to analyze multivariate data. Indian Journal of Microbiology Research. 2023;9(4):241-248.
9. Bakhaidar RB, Naveen NR, Basim P, Murshid SS, Kurakula M, Alamoudi AJ, et al. Response Surface Methodology (RSM) Powered Formulation Development, Optimization and Evaluation of Thiolated Based Mucoadhesive Nanocrystals for Local Delivery of Simvastatin. Polymers. 2022;14(23):5184.
10. Alshweiat A, Abu-Alkebash E, Abuawad A, Athamneh T, Abukhamees S, Oqal M. Preparation and characterization of soluplus-based nanosuspension for dissolution enhancement of indomethacin using ultrasonic assisted precipitation method for formulation and Box-Behnken design for optimization. Drug Development and Industrial Pharmacy. 2024;50(10):878-891.
11. Zhang T, Li X, Xu J, Shao J, Ding M, Shi S. Preparation, Characterization, and Evaluation of Breviscapine Nanosuspension and Its Freeze-Dried Powder. Pharmaceutics. 2022;14(5):923.
12. Younes M, Aquilina G, Engel KH, Fowler P, Frutos Fernandez MJ, Fürst P, et al. Safety evaluation of crosslinked polyacrylic acid polymers (carbomer) as a new food additive. EFSA Journal. 2021;19(8).
13. R. Varges P, M. Costa C, S. Fonseca B, F. Naccache M, De Souza Mendes P. Rheological Characterization of Carbopol® Dispersions in Water and in Water/Glycerol Solutions. Fluids. 2019;4(1):3.
14. Dinkgreve M, Fazilati M, Denn MM, Bonn D. Carbopol: From a simple to a thixotropic yield stress fluid. J Rheol. 2018;62(3):773-780.
15. Akay G, Tong L. Polymer dispersion preparation by flow induced phase inversion emulsification. Part 1 The effect of silica on emulsification and dispersion characteristics. Journal of Materials Science. 2000;35(15):3699-3709.
16. Karakucuk A, Celebi N. Investigation of Formulation and Process Parameters of Wet Media Milling to Develop Etodolac Nanosuspensions. Pharm Res. 2020;37(6).
17. Abla KK, Mneimneh AT, Allam AN, Mehanna MM. Application of Box-Behnken Design in the Preparation, Optimization, and In-Vivo Pharmacokinetic Evaluation of Oral Tadalafil-Loaded Niosomal Film. Pharmaceutics. 2023;15(1):173.
18. Bhattacharjee S. DLS and zeta potential – What they are and what they are not? Journal of Controlled Release. 2016;235:337-351.
19. Ermer J. ICH Q2(R2): Validation of Analytical Procedures. Method Validation in Pharmaceutical Analysis: Wiley; 2025. p. 351-372.
20. Ruiz F, Vallet T, Dufaÿ Wojcicki A, Belissa É, Fontan J-E, de Pontual L, et al. Dosage form suitability in vulnerable populations: A focus on paracetamol acceptability from infants to centenarians. PLoS One. 2019;14(8):e0221261.
21. Ozsoysal S, Heidari H, Guner G, Clancy DJ, Bilgili E. Modeling Power Consumption: A Novel Correlation for Stirred Media Mills with Variable Bead Filling Ratios. Journal of Pharmaceutical and BioTech Industry. 2025;2(3):14.
22. Verma S, Kumar S, Gokhale R, Burgess DJ. Physical stability of nanosuspensions: Investigation of the role of stabilizers on Ostwald ripening. Int J Pharm. 2011;406(1-2):145-152.